YY1 lactylation in microglia promotes angiogenesis through transcription activation-mediated upregulation of FGF2

Xiaotang Wang
The First Affiliated Hospital of Chongqing Medical University, Chongqing Eye Institute
Wei Fan
The First Affiliated Hospital of Chongqing Medical University, Chongqing Eye Institute
Na Li
College of Basic Medicine, Chongqing Medical University
Guoqing Wang
The First Affiliated Hospital of Chongqing Medical University, Chongqing Eye Institute
Siyuan He
The First Affiliated Hospital of Chongqing Medical University, Chongqing Eye Institute
Wanqian Li
The First Affiliated Hospital of Chongqing Medical University, Chongqing Eye Institute
Jun Tan
The First Affiliated Hospital of Chongqing Medical University, Chongqing Eye Institute
Qi Lu
The Children's Hospital of Chongqing Medical University, Chongqing 400016, China
Shengping Hou (sphou828@163.com)
The First Affiliated Hospital of Chongqing Medical University, Chongqing Eye Institute
https://orcid.org/0000-0002-7796-8891

Article

Keywords: ocular neovascularization, retinal microglia, YY1 lactylation

Posted Date: September 24th, 2021

DOI: https://doi.org/10.21203/rs.3.rs-910016/v1

Abstract

Ocular neovascularization is a leading cause of blindness. Retinal microglia have been implicated in hypoxia-induced angiogenesis and vasculopathy, but the underlying mechanisms remain largely unknown. Here, we report that lactylation in microglia is critical for retinal neovascularization. Using lactylome and proteomic analyses, we identified a list of hyperlactylated proteins in the context of increased lactate under hypoxia. Yin Yang-1 (YY1), a transcription factor, is lactylated at lysine 183 (K183) under hypoxia, which is regulated by p300. Furthermore, hyperlactylated YY1 directly enhances fibroblast growth factor 2 (FGF2) transcription and promotes angiogenesis. YY1 mutation at K183 eliminates these effects. Notably, clinical retrospective analysis shows that lactate concentrations in retinopathy of prematurity (ROP) infants are significantly increased compared with those in controls. Taken together, our results demonstrate that YY1 lactylation in microglia promotes FGF2 expression and plays a pivotal proangiogenic role, providing new insights into retinal neovascular diseases.

Introduction

Retinopathy of prematurity (ROP) is a major cause of infantile visual impairments and blindness[1,2]. High oxygen therapy for preterm infants leads to the interruption of normal vessel development and even the loss of well-developed vessels in the retina, since preterm infants have incompletely vascularized retinas. After returning to a typical room air environment, which is relatively hypoxic, the incomplete retinal vascular network cannot meet the increasing metabolic demand. The release of multiple angiogenic factors such as VEGF increases in the hypoxic retina and stimulates pathological vessel formation at the junction between the vascular and avascular areas[1-3]. In addition, the newly-formed vessels are involved in complex retinal pathological changes, including vascular leakage, inflammation, and blood-retinal barrier (BRB) damage, causing the formation of haemorrhages and detachment of the retina, ultimately leading to visual impairments and even permanent blindness[2,4]. Oxygen-induced retinopathy (OIR) is a well-established model of ROP and they exhibit many similar features to each other[5,6].

Microglia, the resident immune cells in the central nervous system (CNS) and retina, have been reported to play crucial roles in angiogenesis and vasculopathy[7-9]. Microglia keep bidirectional communication with endothelial cells (ECs) and are the first immune cells to be activated during hypoxia[10]. Retinal hypoxia leads to pathological angiogenesis and microglia are attracted to the site, localize closely with newly formed vessels and act as important regulators[8,11]. Activated microglia participate actively in the development of OIR, and exert different functions at different stages[8]. Recently, a specific $RIP3^{+}$ subpopulation of microglia was identified and proved to contribute to retinal angiogenesis[7]. Inhibiting microglia activation by minocycline or reducing microglia numbers by clodronate liposomes both delayed the retinal neovascularization process, with no behavioral or cognitive abnormalities[9]. Previous evidence indicates the pivotal proangiogenic role of microglia, but the molecular mechanism remains obscure.

Lactate, a compound produced during the Warburg effect, was previously defined as an energy source and metabolic byproduct that can be generated under hypoxic conditions. Recently, some new functions of lactate have been continuously discovered, including modulation of macrophage polarization, T-cell activation and angiogenesis[12-15]. Lactylation is a novel lactate-derived posttranslational modification (PTM) of histone proteins originally identified by Zhang et al[16]. It functions as a vital epigenetic regulator in many cellular processes. For example, evidence has shown that lactylation can regulate macrophage polarization during bacterial infection, accelerate tumorigenesis of ocular melanoma and facilitate cellular reprogramming[16-19]. However, the role of lactylation in angiogenesis has not been clarified. Since most retinal vasculopathies are induced by hypoxia, including OIR, lactylation is very likely to be involved in retinal neovascularization and exploring the mechanism is of vital importance.

In the current study, we demonstrate that hypoxia-induced lactate production plays pivotal roles in angiogenesis, and that hyperlactylation in microglia promotes retinal neovascularization. We performed lactylome and proteomic analyses and found 67 hyperlactylated proteins in microglia under hypoxia. Among these, we focused on the transcription factor YY1. Our results show that lactylation of YY1 is increased in response to hypoxia and it's regulated by p300. YY1 directly binds to the promoter of FGF2 and promotes FGF2 transcriptional activity with hyperlactylation. Furthermore, hyperlactylated HMC3 cells upregulate the expression of FGF2 and accelerate the proliferation, migration, and tube formation of retinal capillary endothelial cells. Clinically, the retrospective analysis indicates that ROP is associated with upregulated lactate content in blood. Collectively, we evaluate the mechanistic linkage between hypoxia, lactylation, and microglia-mediated neovascularization and provide new insights into retinal vascular disease.

Results

Microglia depletion by the colony stimulating factor 1 receptor (CSF1R) inhibitor PLX3397 suppresses retinal neovascularization

To evaluate whether microglia are involved in the vascular pathogenesis of retinopathy, a double immunofluorescent staining technique was used in retinal flat mounts. The OIR mouse model that recapitulates ROP was developed as the flow chart shows (Fig. 1a). In this model, room air was supplied from the day of birth (P0) to the 7th postnatal day (P0–P7), and then 75% oxygen was supplied from P7-P12 to maintain a high-oxygen environment and room air was supplied until P17 to induce a relatively hypoxic environment as previously described[20]. After modelling, compared with that in the control group, a higher number of microglia gathered around the site of neovascularization in the OIR group (Fig. 1b), indicating a significant functional role for microglia in angiogenesis. To determine whether microglia depletion could affect OIR progression, we utilized a CSF1R inhibitor (PLX3397), which was shown to induce significant microglial ablation[21,22]. The dosing flow chart is shown in Fig. 1c (injection from P10 until P17). After administration, we found that the angiogenesis was greatly suppressed along with the

depletion of microglia (Fig. 1d). Collectively, these results demonstrate the important role of microglia in retinal vascularization.

Elevated lactate and lactylation levels are associated with retinal neovascularization

ROP is a severe vision-threatening disease that may cause childhood blindness worldwide. With improved neonatal care, the survival rate of premature infants has been greatly increased, but the incidence of ROP has also increased[23,24]. We compared the lactate content in the arterial blood of ROP infants with non-ROP infants by arterial blood gas analysis, which is a regular test for premature infants. We found that lactate was significantly increased in ROP infants compared with the control group (Fig. 2a, Supplementary Table 1). This indicates that lactate may be a significant risk factor for ROP.

Lactylation is derived from lactate and participates in multiple cellular processes[16,17]. First, to confirm whether lactylation is involved in proliferative retinopathies induced by hypoxia, we investigated the lactate content and pan lysine lactylation (Pan-Kla) levels in the whole retina of OIR mouse model. Compared with the control group, the production of lactate increased significantly on P17 in the OIR group (Fig. 2b). Pan-Kla levels in retinas were also upregulated at P17 of OIR as shown by Western blotting (Fig. 2c). To confirm whether the lactylation of microglia plays an important role in retinal vascular disease, we used immunofluorescence double staining to analyse the retinal flat mounts. Compared with the control group, lactylation was observed at P17 of OIR, and lactylation colocalized with microglia in the retina as shown by the immunofluorescence results in Fig. 2d. It is worth noting that, the level of Pan-Kla in the retina was relatively downregulated with the use of PLX3397 (Fig. 2e), indicating the important role of lactylation in microglia.

To examine whether lactylation plays a direct role in the vascular pathogenesis of retinopathy, we applied two compounds for in vivo verification experiments, sodium dichloroacetate (DCA) and rotenone, which have been shown to regulate lactylation in cells[16]. DCA can reduce the production of lactate by inhibiting the activity of pyruvate dehydrogenase and rotenone is an inhibitor of the mitochondrial respiratory chain complex that makes cells tend to undergo glycolysis and increases the content of lactate. After compound treatment, the results of the OIR model showed lower lactate and lactylation levels in the DCA group, but increased lactate and lactylation levels in the rotenone group (Fig. 2f-g). Immunofluorescence analysis of retinal flat mounts revealed that the neovascular disease was attenuated to a certain extent after DCA treatment, but aggravated in the rotenone group (Fig. 2h).

Hyperlactylation in HMC3 microglial cells promotes angiogenesis in vitro

Since hypoxia triggers the process of angiogenesis, we exposed HMC3 cells to hypoxia to explore the role of lactylation in microglia. As the degree of hypoxia increased, the lactate content of HMC3 cells

increased, and the level of lactylation was also elevated, especially the protein in the range of 55-70KD (Fig. 3a, b). The proliferation and migration of endothelial cells are vitally important for the formation of vascular networks. We wondered whether microglia with increased lactylation could influence the angiogenesis abilities of human retinal microvascular endothelial cells (HRMECs). We cocultured HMC3 microglial cells from normoxic or hypoxic groups with HRMECs. As the hypoxia time of HMC3 cells increased, the tube formation, migration and proliferation of HRMECs were crucially enhanced (Fig. 3c-e). To further confirm the significant role of the lactate/lactylation levels of microglia in the pathogenesis of angiogenesis. HMC3 cells were treated with DCA and rotenone and then the levels of lactate/lactylation were measured. The lactate/lactylation levels of HMC3 cells were decreased in the DCA group, and increased in the rotenone group (Fig. 3f, g). We also cocultured HMC3 microglial cells from the DCA/DMSO/rotenone groups with HRMECs to explore the influence on HRMECs. The tube formation, migration and proliferation abilities of HRMECs cocultured with HMC3 cells in the DCA group were weakened, while enhanced in the rotenone group (Fig. 3h-j). These results showed that elevated lactylation in HMC3 cells is responsible for promoting the angiogenesis ability of HRMECs.

The lactylation of YY1 in microglia plays an important role in regulating angiogenesis

To characterize the landscape of lactylation in microglia under hypoxia, we treated HMC3 cells with normoxia or 1%O_2 for 24 hrs and then applied lactylome analysis by the 4D lable-free platform method to identify the differentially lactylated proteins. We identified 67 proteins with increased lactylation and 162 proteins with decreased lactylation under hypoxic conditions as differentially expressed lactylated proteins (DELPs) (Supplementary Fig. 1a). The relative quantification of the top 10 proteins with increased lactylation in the Hypoxia-24hrs group are shown in Fig. 4a. Cluster analysis of the identified DELPs was performed to characterize the function of these lactylated proteins. The classification analysis indicated that most of the DELPs exert functions in the nucleus (Supplementary Fig. 1b), and have a potential role in regulating DNA transcription as Fig. 4b shows. Using the Search Tool for the Retrieval of Interacting Genes/Proteins (STRING) database, the protein interaction networks of DELPs suggested that the DELPs mainly function in the binding process, which corresponds with enriched pathways (Fig. 4c). Among these DELPs, YY1 immediately caught our attention since its lactylation level was largely upregulated and it is a multifunctional transcription factor that has a certain regulatory effect on angiogenesis[25]. The proteomic analysis identified only one lactylated lysine residue in YY1 (K183), showing a characteristic tandem mass spectrometry (MS/MS) spectrum including C-terminal y-ions and amino-terminal b-ions (Fig. 4d). To verify whether YY1 lactylation was regulated under cellular stress, HMC3 cells were treated with normoxia or hypoxia for 24 hours. Consistent with the sequencing results, YY1 lactylation was largely increased under hypoxia with no difference in YY1 expression level (Fig. 4e). The colocalization of YY1 and Pan-Kla observed with double-labelled immunofluorescence also confirmed the results (Fig. 4f). We next mutated lysine (K)183 of HMC3 to arginine (R), which mimicked the delactylated state of the protein, by transfecting HMC3 cells with lentivirus containing cDNA of the Flag-tagged YY1 WT or YY1 K183R mutant. Both the WT and K183R mutant groups overexpressed YY1

(Supplementary Fig. 1c, d). Immunoprecipitation of Flag-YY1 followed by immunoblotting for Pan-Kla confirmed that YY1 was lactylated, and that YY1 lactylation levels were decreased in K183R mutant hypoxia-treated HMC3 cells (Fig. 4g). Compared with the WT group, HRMECs cocultured with K183R mutant HMC3 showed weakened tube formation, migration and proliferation capabilities compared with WT groups (Fig. 4h-j). Taken together, these data indicate that lactylation of YY1 at K183 in microglia promotes angiogenesis.

YY1 lactylation contributes to angiogenesis by regulating the expression of FGF2

To identify the potential angiogenic genes that are involved in microglia-mediated angiogenesis, we reverse-transcribed mRNA isolated from normoxic, hypoxic and microglia-depleted retinas in vivo and HMC3 cells in vitro and compared the expression levels of some classic angiogenic-related genes (VEGFA/FGF2/MMP9/MMP2/ANGPTL6)[26-30]. Compared with those in the normoxia group, the FGF2 and VEGFA mRNA expression levels were significantly elevated in OIR mice, while only FGF2 levels decreased notably at both mRNA and protein levels after microglia depletion (Fig. 5a, c). Similarly, hypoxia increased FGF2 mRNA expression within 12 hrs of hypoxia exposure, and the levels remained elevated until 24 hrs in HMC3 cells (Fig. 5b, d). Consistent with previous studies, these results indicate that FGF2 may be the key proangiogenic factor in microglia-mediated neovascularization[7]. DCA and rotenone were used in vivo and in vitro experiments to explore whether lactate/lactylation affects angiogenesis by regulating the expression of angiogenic factors. In the OIR model treated with DCA and rotenone, the expression of FGF2 was decreased in the DCA group, but increased in the rotenone group at P17 (Supplementary Fig. 2a). The similar results were found in HMC3 cells exposed to hypoxia with DCA or rotenone (Supplementary Fig. 2b). Previous studies suggest that YY1 was involved in angiogenesis[25,31]. YY1 contains four C2H2 zinc fingers that are used to bind a specific DNA sequence which located in many promoters and enhancers, promoting or repressing transcription[32,33]. To explore the potential target genes of YY1, we searched three databases, TRANSFAC, Harmonizome and the Cistrome Data Browser, and found that YY1 directly binds to the promoter of FGF2 (Figure 5E)[34]. We found three potential YY1 binding sites of the FGF2 promoter from the JASPAR website and ChIP-qPCR showed that YY1 can bind to the region of -1336 to -1172 bp upstream of the transcription start site of the FGF2 (Fig. 5f, g, Supplementary Fig. 2d). The specificity of the primers used in ChIP-qPCR was verified by NCBI BLAST. A dual-luciferase reporter system was applied to verify the result that YY1 directly promotes the transcription of FGF2 under hypoxia and that mutation at the lactylation site of YY1 resulted lower transcription ability (Fig. 5i). These results indicate that YY1 directly promotes the transcription of FGF2 and this function is regulated by lactylation. After the lactylation site of YY1 was mutated, we detected lower expression of FGF2 at both the mRNA and protein levels following decreased lactylation levels of YY1 (Fig. 5h, Supplementary Fig. 2c). Moreover, reduced lactylation of YY1 in microglia significantly suppressed the angiogenesis of HRMECs (Fig. 4h-j). Collectively, our findings suggest that FGF2 released

from hypoxic microglia is regulated by the lactylation of YY1 and plays an important role in hypoxia-induced angiogenesis.

Inhibiting p300 reduces the lactylation of YY1 and suppresses angiogenesis

Lysine acylation is a series of universal and evolutionarily conserved PTMs[35]. Lactylation is a new form of them and these different forms may share the same writers and erasers. To identify the regulators responsible for modulating lactylation levels in HMC3, we detected the expression patterns of the known acylation modification writers (Tip60, p300 and PCAF) and erasers (HDAC6 and SIRT1)[36,37]. Western blotting assays revealed that p300, HDAC6 and SIRT1 levels were significantly upregulated and Tip60 levels were slightly upregulated in HMC3 cells under hypoxia compared to the respective control cells (Fig. 6a, Supplementary Fig. 3a). However, we detected that only p300 and YY1 were combined with each other according to the Co-IP results (Fig. 6b, Supplementary Fig. 3b). The colocalization of p300 and YY1 was shown by double-label immunofluorescence (Fig. 6c). Previous evidence suggested that p300 is a potential Kla writer protein[16]. To further explore the role of p300 in regulating lactylation levels, the p300 inhibitor A-485 was used in subsequent experiments.A-485 was proved to be a CoA competitive catalytic inhibitor of p300 and L-lactyl-CoA is indispensable for lactylation[38] .The results showed that the lactylation of HMC3 was significantly reduced, and the expression level of FGF2, the hypothetical target of transcriptional regulation of YY1, was also significantly downregulated after A-485 treatment (Fig. 6d). In particular, after HMC3 microglia were treated with A-485, IP and subsequent Western blotting showed decreased lactylation levels of YY1 in these cells compared with control cells (Fig. 6e). The tube formation, migration and proliferation abilities of HRMECs cocultured with HMC3 cells in the A-485 group were weakened (Fig. 6f-h). The results indicate that inhibiting p300 can reduce the lactylation level of YY1 and suppress neovascularization.

Discussion

The functional vascular network in the retina is essential for normal vision. Many vision-threatening diseases are caused by proliferative vasculopathies, including retinopathy of prematurity (ROP), proliferative diabetic retinopathy (PDR) and wet age-related macular degeneration (wAMD)[39,40]. However, the current therapies are quite limited, indicating the urgent need to elucidate mechanisms and discover new therapy targets. In this study, we identified the lactate/p300/YY1 lactylation/FGF2 transcription axis as part of an important mechanism underlying microglia-mediated neoangiogenesis. Mechanistically, hypoxia promotes the production of lactate and the expression of p300 for YY1 lactylation in microglia, which directly activates FGF2 transcription. Our findings present a previously undefined regulatory mechanism in which the expression of FGF2 is modulated by YY1(K183) lactylation. Upregulation of YY1 lactylation enhances FGF2 expression and promotes the angiogenesis of HRMECs, while mutation at the YY1 lactylation site reverses this effect (Fig.7) Whether YY1 requires additional transcription factors or transcription coregulators to drive FGF2 transcription is worthy of further investigation.

Numerous studies have shown that microglial cells contribute to angiogenesis in the brain and retina[41-43]. In pathological angiogenesis, the microglial cells that are highly glycolytic are spatially adjacent to endothelial cells (ECs)[42]. Although the important roles of microglia/macrophages in neovascularization have been established for many years, the mechanisms by which they associate directly with nascent vessels and participate in microenvironment interactions remain largely unknown. Microglia can sense physiological and pathological clues, investigate the surrounding microenvironment and secrete various cytokines and neurotrophic factors when activated. Our data demonstrated that highly glycolytic microglia are regulated by lactylation, and induce FGF2 expression, thereby promoting angiogenesis.

YY1 is a multifunctional transcription factor that is able to repress, activate, and initiate transcription relying upon promoter architecture and the cellular status. For example, YY1-mediated ZNF322A transcription regulation was eliminated when two YY1 binding sites were depleted at -462 ~ -363 in the Del-ZNF322A-pGL4 promoter used for the promoter activity assay[44]. Previous studies have reported that the 30 amino acids between 170 and 200 of YY1 constitute a repressor domain[33,45,46]. When the structure of the repressor domain changes and its repression activity is lost. In the cell, YY1 can be transformed into an activating factor only after the N-terminal activation domain is unmasked and exposed under certain conditions[46-49]. Consistent with our conjecture, the lactylation of the lysine at position YY1 183 may cause the inhibition mechanism to fail and activate the transcriptional activity of YY1, but this hypothesis still needs further investigation. To date, a variety of PTMs have been shown to be involved in regulating the transcriptional activity of YY1, such as acetylation and phosphorylation[45,50,51]. Our research has shown that the transcriptional activity of YY1 is regulated by lactylation, which provides new insights for PTMs and new directions for the study of disease mechanisms.

Previous experiments have demonstrated that lactylation is an important PTM derived from lactate. The emergence of lactylation has improved our understanding of the function of lactate and its role in a variety of pathophysiological conditions[17,52].For example, histone lactylation can directly promote gene transcription, and induce the polarization of macrophages from M1 to M2[16].Lung myofibroblasts promote the profibrotic activity of macrophages by inducing histone lactylation in the promoters of the profibrotic genes in macrophages[53]. Although some studies have shown that lactylation of histones plays an important role in transcription-related functional regulation, we need to further explore whether lactylation of nonhistone proteins matters and how it works. Our data showed that lactylation at lysine 183 of the nonhistone protein YY1 leads to an increase in the transcriptional ability of YY1, directly upregulates the expression of FGF2 and promotes angiogenesis, supporting the idea that the lactylation of nonhistone proteins can also exert important functions and influence cellular processes. The clinical data also suggested the important role of lactate in ROP, but whether it works through lactylation needs further investigation.

We speculated whether the lactylation is similar to the acylation modification that can be directly regulated by some writers and erasers. Our results showed the potential activity of p300 as a Kla writer in

cells. Consistent with previous studies, the transcriptional regulator p300 can directly interact with YY1[54].We inhibited p300 in HMC3 cells with A485 and observed decreased lactylation levels of YY1. These data suggest that p300 can regulate the lactylation level of YY1.

Overall, this study revealed that the K183 lactylation level of YY1 in microglia is increased in response to hypoxia. YY1 lactylation promotes FGF2 expression through transcriptional activation, and further contributes to endothelial cell proliferation, migration and tube formation. YY1-K183 lactylation can be a potential predictive marker for pathological angiogenesis. Furthermore, p300 affects angiogenesis by targeting YY1 lactylation and it can be a potential target. These findings expand the field of protein epigenetic regulation and provide potential targets for pathological angiogenesis therapy.

Methods

Antibodies and reagents

The following antibodies and reagents were used:CD31 (Abcam, ab9498); Iba1 (WAKO019-19741); Pan-Kla (PTM-1401); YY1 (Proteintech, 66281-1-lg); YY1 (Cell Signaling, 46395S); FGF2 (Santa Cruz, sc74412); p300 (Santa Cruz, sc48343); HDAC6 (Santa Cruz, sc28386); SIRT1 (Abcam, ab7343); PCAF (Abcam, ab12188); TIP60 (Santa Cruz, sc166323); β-Actin (Proteintech, 20536-1-AP); Ki67 (Abcam ab16667); Rotenone (Rhawn, R006873); Sodium Dichloroacetate (DCA, Rhawn, R052025); Crystal violet (Solarbio, G1062); Matrigel (BD, 356234)Alexa Fluor 488-labelled Goat Anti-Rabbit IgG(H+L) (Beyotime, A0423); Alexa Fluor 488-labelled Goat Anti-Mouse IgG(H+L) (Beyotime, A0428); Cy3-labelled Donkey Anti-Goat IgG(H+L) (Beyotime, A0502); Cy3-labelled Goat Anti-Mouse IgG (H+L) (Beyotime, A0521); Cy3-labelled Goat Anti-Rabbit IgG (H+L) (Beyotime, A0516).

Animal experiments

C57BL/6J mice obtained from the Experimental Animal Center of Chongqing Medical University (Chongqing, China) were housed in a specific pathogen-free facility. All protocols were approved by the Ethics Committee of the First Affiliated Hospital of Chongqing Medical University (Number: 2019-101) and conformed to the ARVO Statement for the Use of Animals in Ophthalmic and Vision Research.

Induction of OIR

OIR is a model of ROP, which is characterized by the late stage of destructive pathological angiogenesis.C57BL/6J pups were defined as P0 when they were born. The pups and suckling mice received food and water freely with a 12/12 hrs-day/night cycle in normal air for 7 days (P0-P7). On day P7, healthy pups and suckling mice were placed into a glass oxygen chamber together (Chenxi dianzi;

Zhejiang; China), with the oxygen flow controlled to 0.50-0.75 L/min and the oxygen concentration was maintained at (75±2) %. The animals were kept in a glass oxygen chamber for five consecutive days. At P12, the pups were returned to a normal air environment and continually co-bred with the suckling mice for five days, The pups were sacrificed at the age of P17 and the retinas were removed for subsequent experiments.

Microglia depletion

For microglia depletion using PLX3397 (MedChemExpress), mice were injected with PLX3397 from P10 to P17. PLX3397 was diluted in 1% dimethyl sulfoxide (DMSO), 45% polyethylene glycol 300 (PEG-300), 5% Tween 80 and saline. After injection, no obvious behavioural or health problems were observed.

Cell lines and cell cultures

HMC3 cells (ATCC; Manassas, VA, USA) were cultured in EMEM containing 10% fetal bovine serum (FBS; Gibco) and 1% penicillin/streptomycin with 5% CO2 at 37°C. HRMECs (Cell Systems; Seattle, America) were cultured in Complete Classic Medium with Serum & CultureBoost (Cell Systems) at 37 °C in under 5% CO2. For coculture experiments, HMC3s were precultured under the corresponding conditions for 24 hours and then cocultured with HRMECs.

Quantification of lactate level

The LA Assay Kit (Solarbio) was used to determine the content of lactate in retina tissues and cell lysates. Briefly, lactate extracted from different treatment groups was combined into 96-well-plates, followed by the addition of reducing agent solution and the reduction reaction colour developing solution. The lactate content was determined by detecting the absorbance at 570 nm. Each experiment was repeated three times.

Immunofluorescence

Eyes obtained on day of P17 were placed into 4% paraformaldehyde for 2 hrs. Then the retinas were sheared into flat mounts and blocked with a 5% goat serum and 0.4% TritonX-100 for 1 hr, followed by incubation with primary antibodies at 4°C overnight. Then the retinas were washed carefully and incubated with secondary antibody combinations for 1 hr. Images were taken by confocal microscopy (Zeiss, Germany). CellSens Dimension software was used to estimate the number of microglia (Iba1).

Quantitative real-time PCR

RNA was isolated using TRIzol reagent from HMC3 cells (1×10^6 cells) or retinal tissue. cDNA was generated by the RT Master Mix for qPCR (MCE, USA). Real-time qPCR was performed using the SYBR Green qPCR Master Mix (MCE, USA) with the ABI Prism 7500 system (Applied Biosystems, CA, United States). The specific primers were synthesized by Shanghai Sangon Co. Ltd (Shanghai, China), and the PCR primers employed are listed in Supplementary Table 2. All of the reactions were performed at least in triplicate with β-actin as the control.

Western blotting

The same amount of protein (30 μg) was separated by 8–12% SDS-PAGE and transferred onto PVDF membranes (Millipore, MA, USA). The membranes were blocked with 5% skim milk, followed by incubation with primary antibodies overnight at 4 °C and secondary antibodies for 1 hr respectively. The signals were detected using an ECL kit (Advansta, CA, USA) and quantified with Image J software. VeriBlot for IP Detection Reagent (HRP)(Abcam), a special secondary antibody, was used for IB after IP.

In vitro lentivirus infection and plasmid transfection

HMC3 cells were seeded in 6-well-plates at over 60% confluence and used for lentivirus infection. Lentiviruses subcloned with cDNA of Flag-tagged YY1 WT or YY1 K183R mutant which were constructed and purchased from Shanghai Genechem Co, Ltd, were added at an MOI of 30 for 8 hrs. The medium was replaced after 8hrs and the cells were used for further experiments. The plasmids used for luciferase activity assays were constructed and purchased from Shanghai Genechem Co, Ltd and transfected into HMC3 cells by Lipofectamine™ 2000 (Invitrogen, 11668019).

Pan antibody-based PTM enrichment

HMC3 cells were treated with hypoxia or normoxia for 24 hrs. To enrich Kla modified peptides, the tryptic peptides were dissolved in NETN buffer (1 mM EDTA, 50 mM Tris-HCl,100 mM NaCl, 0.5% NP-40, pH 8.0), followed by incubation with prewashed beads (PTM Bio) at 4°C for 12hrs. Trifluoroacetic acid (0.1%) was used to elute the bound peptides. The eluted peptides were vacuum-dried and desalted with C18 ZipTips (Millipore) for LC-MS/MS analysis.

LC-MS/MS Analysis and Database Search

LC-MS/MS analysis was supported by Jingjie PTM BioLabs (Hangzhou, China). In brief, the tryptic peptides were dissolved in solvent A (0.1% formic acid, 2% acetonitrile/ in water) and separated by a home-made reversed-phase analytical column (25 cm length, 100 μm i.d.) on a nanoElute UHPLC system (Bruker Daltonics). After being subjected to a capillary source, the peptides were conducted with the timsTOF Pro (Bruker Daltonics) mass spectrometry for further analysis in parallel accumulation serial fragmentation (PASEF) mode. The MS/MS data were processed by the MaxQuant search engine (v.1.6.6.0). Tandem mass spectra were searched using the human SwissProt database (20366 entries) and reverse decoy database. FDR< 1%. The relative quantitative values of modified peptides in different samples are obtained by centralizing the signal intensity values in different samples. After filtering lysine lactylation sites (localization probability >0.75), the relative quantitative values of each sample were obtained by two experiments. All the ratios of quantified lysine lactylation peptides were normalized according to their corresponding protein expression levels. The protein pathways were annotated using KEGG database. The STRING database was used to identify protein-protein interactions of the DELPs

Co-Immunoprecipitation (Co-IP)

An immunoprecipitation kit (Abcam, ab206996) was used for immunoprecipitation of the corresponding proteins. Following the manufacturer's instructions, the lysates of cells were incubated with antibody for 12 hrs at 4℃. 40 μl protein A/G beads were prewashed and then incubated with beads for another 2 hrs. After extensive washing, bound proteins were processed by Western blotting using the corresponding antibodies.

ChIP assay

The ChIP assay was performed using SimpleChIP Plus Enzymatic Chromatin IP Kit (CST, 9004S). Briefly, 1×10^7 HMC3 cells after fixation were resuspended in ChIP buffer containing 1 × Protease Inhibitor Cocktail (CST). Then, micrococcal nuclease was used to shear chromatin DNA into fragments ranging between 150 and 900 bp. The DNA fragments were immunoprecipitated with 10 μl precleared protein A/G agarose beads overnight at 4°C with anti-YY1 (CST, 46395S) or anti-IgG (CST, 3900) antibodies. YY1 occupancy on the FGF2 promoter was examined using RT-quantitative PCR analysis. The ChIP-qPCR primers employed are listed in supplementary Table 2.

Luciferase Activity Assays

The FGF2 promoter region was cloned into the luciferase reporter vector.YY1 WT and K183R HMC3 cells and control HMC3 cells were seeded in 96-well plates and cotransfected with the constructed plasmids. After 24 hrs in normoxia, the cells were transferred to hypoxia for another 24 hrs. A dual-luciferase reporter gene assay kit (Promega, E2920) was used to detect the luciferase activities. Renilla luciferase activity was used to normalize reporter gene activities.

HRMECs tube formation assay

Endothelial cell tube formation ability was evaluated by Matrigel purchased from Corning. Briefly, 50 μl Matrigel was placed into each well of 96-well plates and incubated at 37°C for 40 mins in a 5% CO2 incubator. Microglia were exposed to different treatments for 24 hrs. A total of 2.0×10^4 HRMECs were seeded per well on the Matrigel and cocultured with pretreated microglia. Tube formation at the indicated times of 12 and 20 hrs was acquired by microscopy. We captured three random images per well and Image-Pro Plus software was used to measure the length of the tubes. Each experiment was repeated three times and at least three wells per condition.

HRMEC migration assay

The migration of HRMECs was assayed using 24-well Transwell chambers with 8-μm pore size filters (Corning, 3422). Briefly, microglia were seeded in the bottom chamber and pretreated for 24 hours. Then 1.5×10^4/ml HRMECs were placed onto the upper chamber and cocultured at 37°C under 5% CO_2 for 24 hrs. After fixation with 4% paraformaldehyde for 30 minutes, HRMECs were stained with 1% crystal violet. The number of the cells migrating to the bottom side of the filter was counted after wiping away the cells on the upper surface. Five images were captured per well under a microscope screening station (scanR, OLYMPUS, Tokyo, Japan), and the cells were counted by three investigators. Each experiment was repeated three times.

HRMEC proliferation assay

The proliferation of HMRECs was assayed using 24-well Transwell chambers with 0.3-μm pore size filters (Corning, 3413). Briefly, microglia were exposed to different treatments for 24 hrs. Then 2.0×10^4/ml HRMECs were placed in the bottom chamber and cocultured with the pretreated microglia for 24 hrs at 37°C under 5% CO2. After fixation with 4% paraformaldehyde for 30 minutes, the proliferating cells were stained with Ki67. Five images were captured per well.

Clinical retrospective study

The clinical retrospective study included 121 preterm infants (28~33 weeks of gestational age) who were admitted to the Children's Hospital of Chongqing Medical University between June 2019 and July 2021 (matching criteria: sex, age, weight, gestational age, birth weight, multiple birth, ethnic group). We excluded preterm infants who were suffering extremely serious diseases, such as multiple organ failure, cardiac arrest, septicemia and respiratory diseases that may directly influence the concentration of lactate in blood, such as acute respiratory distress syndrome, respiratory failure and severe pneumonia. ROP diagnostic examinations were performed using indirect ophthalmoscopy. Levels of blood lactate were measured by arterial blood gas analysis prior to commencing artificial ventilation treatment.

Statistical analysis

All data are presented as the mean ± SD and were analysed by SPSS 20.0 software (IBM, Chicago, IL, USA). The normal distribution of the data was confirmed by Shapiro-Wilk and Kolmogorov–Smirnov tests. Student's t-test was used to compare differences between two groups and one-way ANOVA followed by a Bonferroni post hoc test was used for three or more groups. Clinical data analysis was conducted with Mann–Whitney U- test, Fisher's exact test, or $\chi 2$-test on various parameters. * Denotes $p < 0.05$, ** denotes $p < 0.01$ and *** denotes $p < 0.001$, which were considered statistically significant between groups.

Data availability

Any further data not included in the manuscript is available from the corresponding author on reasonable request.

References

1 Hellstrom, A., Smith, L. E. & Dammann, O. Retinopathy of prematurity. *Lancet* **382**, 1445-1457, doi:10.1016/S0140-6736(13)60178-6 (2013).

2 Hartnett, M. E. & Penn, J. S. Mechanisms and management of retinopathy of prematurity. *N Engl J Med* **367**, 2515-2526, doi:10.1056/NEJMra1208129 (2012).

3 Kandasamy, Y., Hartley, L., Rudd, D. & Smith, R. The association between systemic vascular endothelial growth factor and retinopathy of prematurity in premature infants: a systematic review. *Br J Ophthalmol* **101**, 21-24, doi:10.1136/bjophthalmol-2016-308828 (2017).

4 YH, K. *et al.* Triamcinolone suppresses retinal vascular pathology via a potent interruption of proinflammatory signal-regulated activation of VEGF during a relative hypoxia. *Neurobiology of disease* **26**, 569-576, doi:10.1016/j.nbd.2007.02.002 (2007).

5 Grossniklaus, H. E., Kang, S. J. & Berglin, L. Animal models of choroidal and retinal neovascularization. *Prog Retin Eye Res* **29**, 500-519, doi:10.1016/j.preteyeres.2010.05.003 (2010).

6 Chen, D. Y. *et al.* Endothelium-derived semaphorin 3G attenuates ischemic retinopathy by coordinating beta-catenin-dependent vascular remodeling. *J Clin Invest* **131**, doi:10.1172/JCI135296 (2021).

7 He, C. *et al.* A specific RIP3(+) subpopulation of microglia promotes retinopathy through a hypoxia-triggered necroptotic mechanism. *Proc Natl Acad Sci U S A* **118**, doi:10.1073/pnas.2023290118 (2021).

8 Li, J. *et al.* The phase changes of M1/M2 phenotype of microglia/macrophage following oxygen-induced retinopathy in mice. *Inflamm Res* **70**, 183-192, doi:10.1007/s00011-020-01427-w (2021).

9 Xu, W. *et al.* Microglial density determines the appearance of pathological neovascular tufts in oxygen-induced retinopathy. *Cell Tissue Res* **374**, 25-38, doi:10.1007/s00441-018-2847-5 (2018).

10 Dudvarski Stankovic, N., Teodorczyk, M., Ploen, R., Zipp, F. & Schmidt, M. H. H. Microglia-blood vessel interactions: a double-edged sword in brain pathologies. *Acta Neuropathol* **131**, 347-363, doi:10.1007/s00401-015-1524-y (2016).

11 Boeck, M. *et al.* Temporospatial distribution and transcriptional profile of retinal microglia in the oxygen-induced retinopathy mouse model. *Glia* **68**, 1859-1873, doi:10.1002/glia.23810 (2020).

12 Lee, D. C. *et al.* A lactate-induced response to hypoxia. *Cell* **161**, 595-609, doi:10.1016/j.cell.2015.03.011 (2015).

13 Pucino, V. *et al.* Lactate Buildup at the Site of Chronic Inflammation Promotes Disease by Inducing CD4(+) T Cell Metabolic Rewiring. *Cell Metab* **30**, 1055-1074 e1058, doi:10.1016/j.cmet.2019.10.004 (2019).

14 Zhang, J. *et al.* Endothelial Lactate Controls Muscle Regeneration from Ischemia by Inducing M2-like Macrophage Polarization. *Cell Metab* **31**, 1136-1153 e1137, doi:10.1016/j.cmet.2020.05.004 (2020).

15 Rabinowitz, J. D. & Enerback, S. Lactate: the ugly duckling of energy metabolism. *Nat Metab* **2**, 566-571, doi:10.1038/s42255-020-0243-4 (2020).

16 Zhang, D. *et al.* Metabolic regulation of gene expression by histone lactylation. *Nature* **574**, 575-580, doi:10.1038/s41586-019-1678-1 (2019).

17 Yu, J. *et al.* Histone lactylation drives oncogenesis by facilitating m(6)A reader protein YTHDF2 expression in ocular melanoma. *Genome Biol* **22**, 85, doi:10.1186/s13059-021-02308-z (2021).

18 Irizarry-Caro, R. A. *et al.* TLR signaling adapter BCAP regulates inflammatory to reparatory macrophage transition by promoting histone lactylation. *Proc Natl Acad Sci U S A* **117**, 30628-30638, doi:10.1073/pnas.2009778117 (2020).

19 Li, L. *et al.* Glis1 facilitates induction of pluripotency via an epigenome-metabolome-epigenome signalling cascade. *Nat Metab* **2**, 882-892, doi:10.1038/s42255-020-0267-9 (2020).

20 Smith, L. E. *et al.* Oxygen-induced retinopathy in the mouse. *Invest Ophthalmol Vis Sci* **35**, 101-111 (1994).

21 Elmore, M. R. *et al.* Colony-stimulating factor 1 receptor signaling is necessary for microglia viability, unmasking a microglia progenitor cell in the adult brain. *Neuron* **82**, 380-397, doi:10.1016/j.neuron.2014.02.040 (2014).

22 Sosna, J. *et al.* Early long-term administration of the CSF1R inhibitor PLX3397 ablates microglia and reduces accumulation of intraneuronal amyloid, neuritic plaque deposition and pre-fibrillar oligomers in 5XFAD mouse model of Alzheimer's disease. *Mol Neurodegener* **13**, 11, doi:10.1186/s13024-018-0244-x (2018).

23 Park, J. H., Hwang, J. H., Chang, Y. S., Lee, M. H. & Park, W. S. Survival rate dependent variations in retinopathy of prematurity treatment rates in very low birth weight infants. *Sci Rep* **10**, 19401, doi:10.1038/s41598-020-76472-w (2020).

24 Gunn, D. J., Cartwright, D. W. & Gole, G. A. Incidence of retinopathy of prematurity in extremely premature infants over an 18-year period. *Clin Exp Ophthalmol* **40**, 93-99, doi:10.1111/j.1442-9071.2011.02724.x (2012).

25 Yang, W. *et al.* YY1 Promotes Endothelial Cell-Dependent Tumor Angiogenesis in Hepatocellular Carcinoma by Transcriptionally Activating VEGFA. *Front Oncol* **9**, 1187, doi:10.3389/fonc.2019.01187 (2019).

26 Ash, D. *et al.* The P-type ATPase transporter ATP7A promotes angiogenesis by limiting autophagic degradation of VEGFR2. *Nat Commun* **12**, 3091, doi:10.1038/s41467-021-23408-1 (2021).

27 Fang, J. H. *et al.* MicroRNA-29b suppresses tumor angiogenesis, invasion, and metastasis by regulating matrix metalloproteinase 2 expression. *Hepatology* **54**, 1729-1740, doi:10.1002/hep.24577 (2011).

28 Gordon-Weeks, A. N. *et al.* Neutrophils promote hepatic metastasis growth through fibroblast growth factor 2-dependent angiogenesis in mice. *Hepatology* **65**, 1920-1935, doi:10.1002/hep.29088 (2017).

29 Kuo, T. C. *et al.* Angiopoietin-like protein 1 suppresses SLUG to inhibit cancer cell motility. *J Clin Invest* **123**, 1082-1095, doi:10.1172/jci64044 (2013).

30 Zajac, E. *et al.* Angiogenic capacity of M1- and M2-polarized macrophages is determined by the levels of TIMP-1 complexed with their secreted proMMP-9. *Blood* **122**, 4054-4067, doi:10.1182/blood-2013-05-501494 (2013).

31 Fu, C. Y., Wang, P. C. & Tsai, H. J. Competitive binding between Seryl-tRNA synthetase/YY1 complex and NFKB1 at the distal segment results in differential regulation of human vegfa promoter activity during angiogenesis. *Nucleic Acids Res* **45**, 2423-2437, doi:10.1093/nar/gkw1187 (2017).

32 Shi, Y., Lee, J. S. & Galvin, K. M. Everything you have ever wanted to know about Yin Yang 1. *Biochim Biophys Acta* **1332**, F49-66, doi:10.1016/s0304-419x(96)00044-3 (1997).

33 Thomas, M. J. & Seto, E. Unlocking the mechanisms of transcription factor YY1: are chromatin modifying enzymes the key? *Gene* **236**, 197-208, doi:10.1016/s0378-1119(99)00261-9 (1999).

34 Mei, S. *et al.* Cistrome Data Browser: a data portal for ChIP-Seq and chromatin accessibility data in human and mouse. *Nucleic Acids Res* **45**, D658-D662, doi:10.1093/nar/gkw983 (2017).

35 Figlia, G., Willnow, P. & Teleman, A. A. Metabolites Regulate Cell Signaling and Growth via Covalent Modification of Proteins. *Dev Cell* **54**, 156-170, doi:10.1016/j.devcel.2020.06.036 (2020).

36 Zhao, S., Zhang, X. & Li, H. Beyond histone acetylation-writing and erasing histone acylations. *Curr Opin Struct Biol* **53**, 169-177, doi:10.1016/j.sbi.2018.10.001 (2018).

37 Wang, Z. A. & Cole, P. A. The Chemical Biology of Reversible Lysine Post-translational Modifications. *Cell Chem Biol* **27**, 953-969, doi:10.1016/j.chembiol.2020.07.002 (2020).

38 Lasko, L. M. *et al.* Discovery of a selective catalytic p300/CBP inhibitor that targets lineage-specific tumours. *Nature* **550**, 128-132, doi:10.1038/nature24028 (2017).

39 Chen, M., Luo, C., Zhao, J., Devarajan, G. & Xu, H. Immune regulation in the aging retina. *Prog Retin Eye Res* **69**, 159-172, doi:10.1016/j.preteyeres.2018.10.003 (2019).

40 Bradley, J., Ju, M. & Robinson, G. S. Combination therapy for the treatment of ocular neovascularization. *Angiogenesis* **10**, 141-148, doi:10.1007/s10456-007-9069-x (2007).

41 Uemura, A. *et al.* VEGFR1 signaling in retinal angiogenesis and microinflammation. *Prog Retin Eye Res*, 100954, doi:10.1016/j.preteyeres.2021.100954 (2021).

42 Liu, Z. *et al.* Glycolysis links reciprocal activation of myeloid cells and endothelial cells in the retinal angiogenic niche. *Sci Transl Med* **12**, doi:10.1126/scitranslmed.aay1371 (2020).

43 Li, Z. *et al.* M-CSF, IL-6, and TGF-β promote generation of a new subset of tissue repair macrophage for traumatic brain injury recovery. *Sci Adv* **7**, doi:10.1126/sciadv.abb6260 (2021).

44 Lin, C. C. *et al.* Dysregulated Kras/YY1/ZNF322A/Shh transcriptional axis enhances neo-angiogenesis to promote lung cancer progression. *Theranostics* **10**, 10001-10015, doi:10.7150/thno.47491 (2020).

45 Yao, Y. L., Yang, W. M. & Seto, E. Regulation of transcription factor YY1 by acetylation and deacetylation. *Mol Cell Biol* **21**, 5979-5991, doi:10.1128/MCB.21.17.5979-5991.2001 (2001).

46 Bushmeyer, S. M. & Atchison, M. L. Identification of YY1 sequences necessary for association with the nuclear matrix and for transcriptional repression functions. *J Cell Biochem* **68**, 484-499 (1998).

47 Verheul, T. C. J., van Hijfte, L., Perenthaler, E. & Barakat, T. S. The Why of YY1: Mechanisms of Transcriptional Regulation by Yin Yang 1. *Front Cell Dev Biol* **8**, 592164, doi:10.3389/fcell.2020.592164 (2020).

48 Austen, M., Luscher, B. & Luscher-Firzlaff, J. M. Characterization of the transcriptional regulator YY1. The bipartite transactivation domain is independent of interaction with the TATA box-binding protein, transcription factor IIB, TAFII55, or cAMP-responsive element-binding protein (CPB)-binding protein. *J Biol Chem* **272**, 1709-1717, doi:10.1074/jbc.272.3.1709 (1997).

49 Shi, Y., Seto, E., Chang, L. S. & Shenk, T. Transcriptional repression by YY1, a human GLI-Kruppel-related protein, and relief of repression by adenovirus E1A protein. *Cell* **67**, 377-388, doi:10.1016/0092-8674(91)90189-6 (1991).

50 Rizkallah, R. & Hurt, M. M. Regulation of the transcription factor YY1 in mitosis through phosphorylation of its DNA-binding domain. *Mol Biol Cell* **20**, 4766-4776, doi:10.1091/mbc.E09-04-0264 (2009).

51 Kassardjian, A. *et al.* The transcription factor YY1 is a novel substrate for Aurora B kinase at G2/M transition of the cell cycle. *PLoS One* **7**, e50645, doi:10.1371/journal.pone.0050645 (2012).

52 Xu, H., Wu, M., Ma, X., Huang, W. & Xu, Y. Function and Mechanism of Novel Histone Posttranslational Modifications in Health and Disease. *Biomed Res Int* **2021**, 6635225, doi:10.1155/2021/6635225 (2021).

53 Cui, H. *et al.* Lung Myofibroblasts Promote Macrophage Profibrotic Activity through Lactate-induced Histone Lactylation. *Am J Respir Cell Mol Biol* **64**, 115-125, doi:10.1165/rcmb.2020-0360OC (2021).

54 Tang, W. *et al.* The p300/YY1/miR-500a-5p/HDAC2 signalling axis regulates cell proliferation in human colorectal cancer. *Nat Commun* **10**, 663, doi:10.1038/s41467-018-08225-3 (2019).

Declarations

Acknowledgements

This study was supported by National Natural Science Foundation Project of China (81873678, 82070951), The Innovative Research Group Project of Chongqing Education Commission (CXQT19015), Natural Science Foundation Project of Chongqing (cstc2019jcyjmsxmX0120), the innovation supporting Plan of Overseas Study of Chongqing (cx2018010) and National Key Clinical Specialties Construction Program of China, Chongqing Branch of National Clinical Research Center for Ocular Diseases and Chongqing Key Laboratory of Ophthalmology (CSTC, 2008CA5003).

Author contributions

X.T.W. and F.W. designed and did experiments, analyzed and interpreted data and wrote the manuscript; X.T.W. and F.W. did the investigation; N.L., S.Y.H., W.Q.L and G.Q.W. helped design some experiments; Q.L. provided advice; S.P.H. funded and oversaw the research programme and edited the manuscript. All authors reviewed and approved the final version of the manuscript.

Competing interests: The authors declare no competing interests

Figures

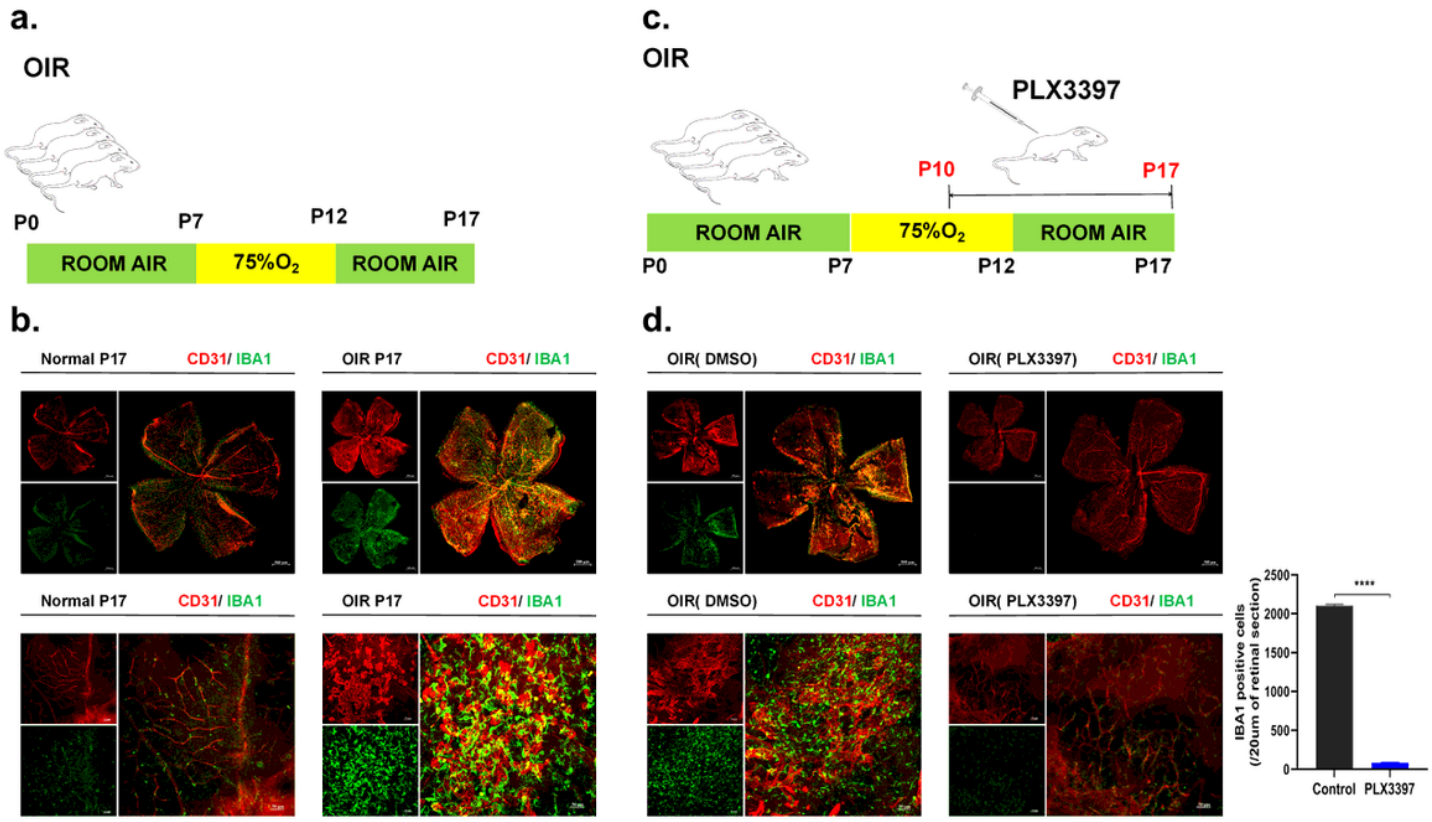

Figure 1

Microglia depletion by the CSF1R inhibitor PLX3397 suppresses retinal neovascularization (a) OIR modelling flow chart. (b) IBA-1 (microglial marker) and CD31 (endothelial cell marker) double stained confocal images of retinas in normoxia control (Normal) and OIR mice (OIR). (c) PLX3397 dosing flow chart. (d) IBA-1 and CD31 double stained retinal flat mounts (OIR (DMSO) and OIR (PLX3397)). The number of IBA1 positive cells was recorded and analysed by cellSens Dimension software.

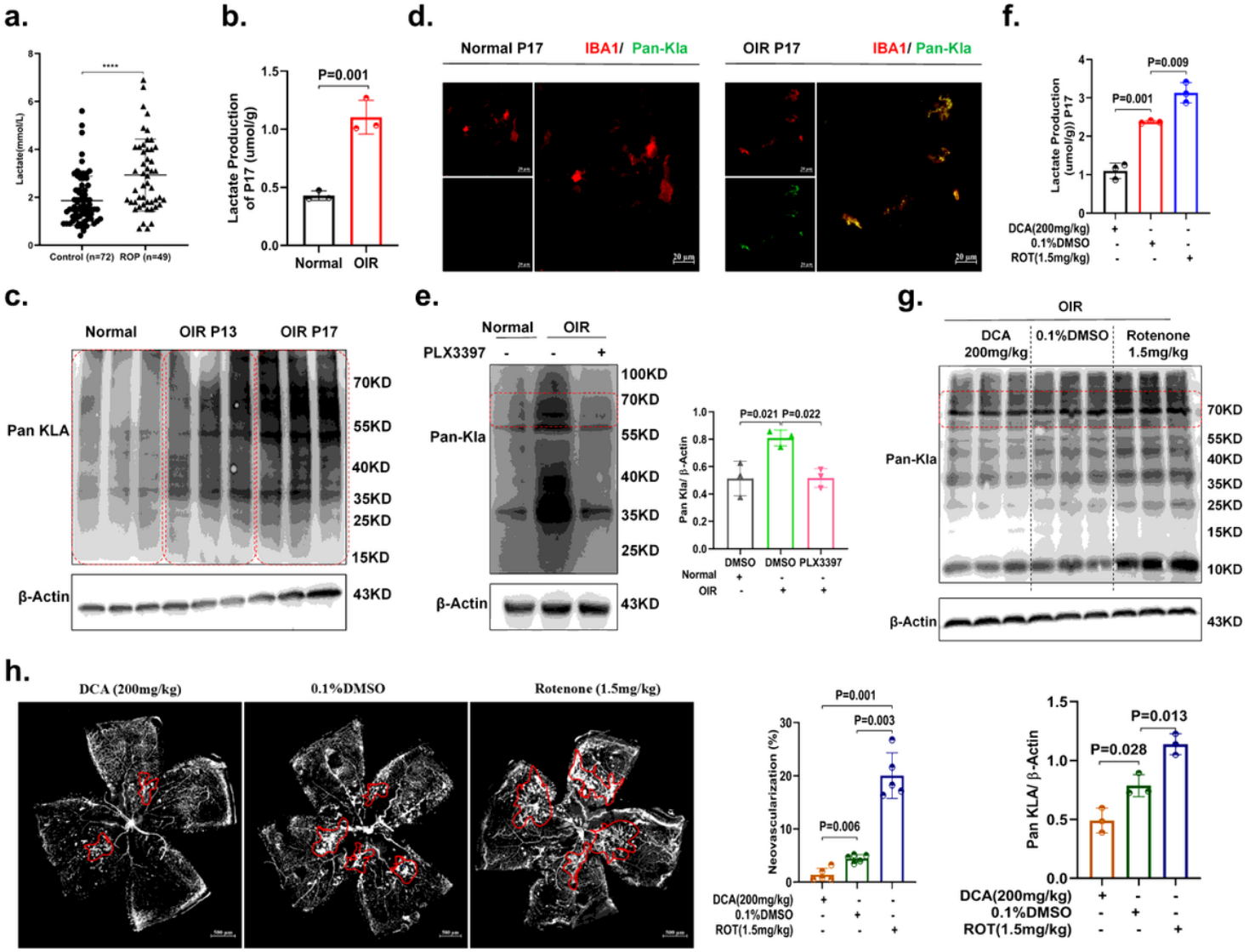

Figure 2

Elevated lactate and lactylation levels are associated with retinal neovascularization (a) Blood lactate quantification for ROP (ROP) and non-ROP (Control) infants. The normal range is between 0.7~2.1 mmol/L. (b) Retinal lactate quantification in normoxia control mice (Normal) and OIR mice (OIR) at P17. (c) Pan-Kla in the retinas of normal control (Normal), OIR (OIR P13) and OIR (OIR P17) mice. (d) IBA-1 and Pan-Kla double stained retinal flat mounts in normoxia control (Normal P17) and OIR mice (OIR P17). (e) Pan-Kla in the retinas of normal control (Normal), OIR (DMSO) and OIR (PLX3397) mice. (f) Lactate production of retinal samples in OIR mice (OIR P17) treated with DCA (200mg/kg), DMSO (0.1%) rotenone(1.5mg/kg). (g) Quantification of Pan-Kla in the retinas of OIR mice (OIR P17) treated with DCA (200mg/kg), DMSO (0.1%) and rotenone(1.5mg/kg) were analysed by Western blotting. (h) Confocal images of CD31-stained retinal flat mounts in OIR P17 mice treated with DCA (200 mg/kg), DMSO (0.1%) and rotenone (1.5 mg/kg). The relative proportion of neovascularization in the retina was calculated and measured by Image J.

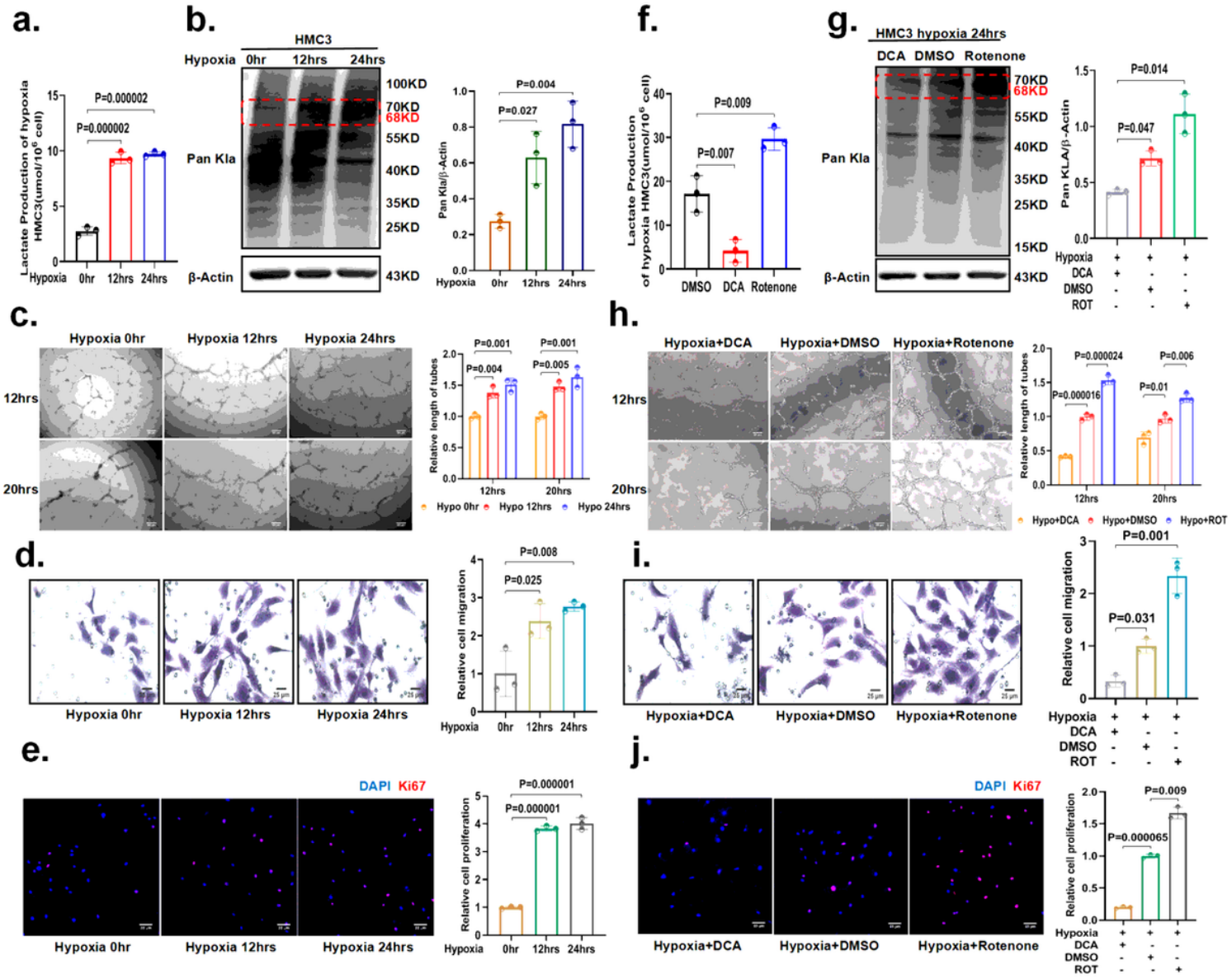

Figure 3

Hyperlactylation in HMC3 microglial cells promotes angiogenesis in vitro (a) Lactate production of HMC3 cells in the three groups treated with hypoxia for 0 hr, 12 hrs and 24 hrs. (b) Quantification of Pan-Kla in the HMC3 cells of hypoxia 0 hr, hypoxia 12 hrs and hypoxia 24 hrs were analyzed by Western blotting. (c) Tube formation analysis. HMC3 cells were pretreated with 1% O2 or normoxia for 24 hrs and then cocultured with HRMECs. Tube formation was assayed 12 hrs and 20 hrs after cell seeding. (n=3, one-way ANOVA, Bonferroni test). Scale bar: 50 μm. (d) HRMECs migration was evaluated by transwell assay. Scale bar: 25 μm. (e) HRMECs proliferation was evaluated by Ki67 staining. Scale bar: 50 μm. (f-g) Quantification of lactate and Pan-Kla in HMC3 cells in the three groups treated with DCA (20mM), DMSO and rotenone(50nM) under hypoxia for 24 hrs. (h-j) HMC3 cells were pretreated with 1% O2 for 24 hrs with DCA, DMSO or rotenone. Then HRMECs were cocultured with the pretreated microglia. The tube formation, migration and proliferation assays were performed as shown in the Methods.

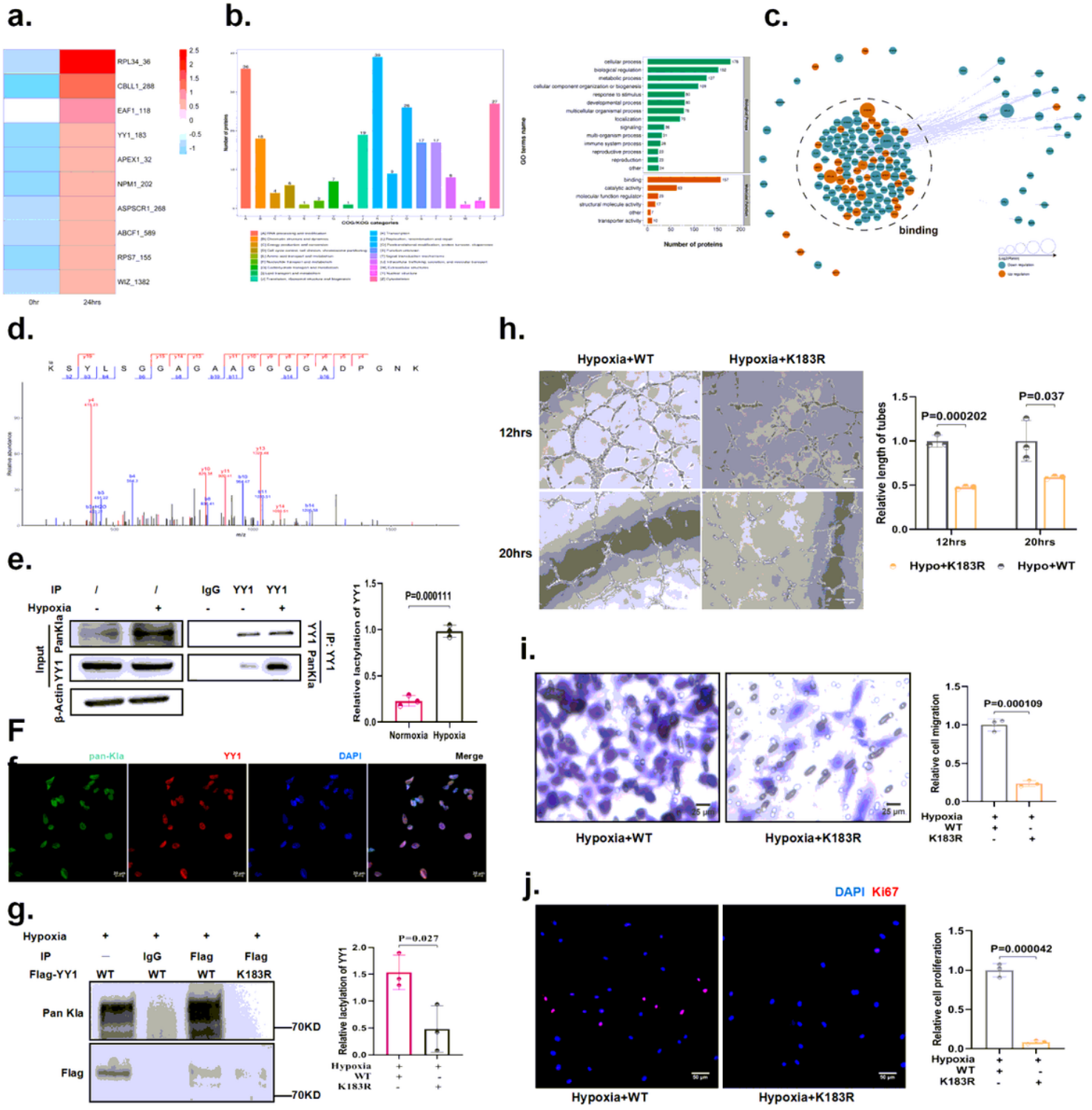

Figure 4

The lactylation of YY1 in microglia plays an important role in regulating angiogenesis (a) Heatmap shows the top 10 DELPs with increased lactylation under hypoxia for 24 hrs. (b) The enrichment analysis of DELPs. (c) Using the STRING database, DELPs specifically target the binding process. The node size corresponds to the relative fold change of lactylation. (d) Collision-induced dissociation (CID) analysis was used to determine the modification sites. The MS/MS spectrum of modified "(Kla)SYLSGGAGAAGGGGADPGNK"is shown. (e) Hypoxia increases YY1 lactylation. Lactylation of YY1

in HMC3 cells under normoxia or hypoxia for 24 hrs was detected by Pan anti-Kla antibody. (f) Co-localization of YY1 and Pan-Kla by double-label immunofluorescence. (g) Mutants of YY1 at K183 shows lower lactylation. (h-j) HMC3 cells overexpressing WT or K183R YY1 were pretreated with 1% O2 for 24 hrs. Then HRMECs were cocultured with the pretreated HMC3 cells. The tube formation, migration and proliferation assays were performed as shown in the Methods.

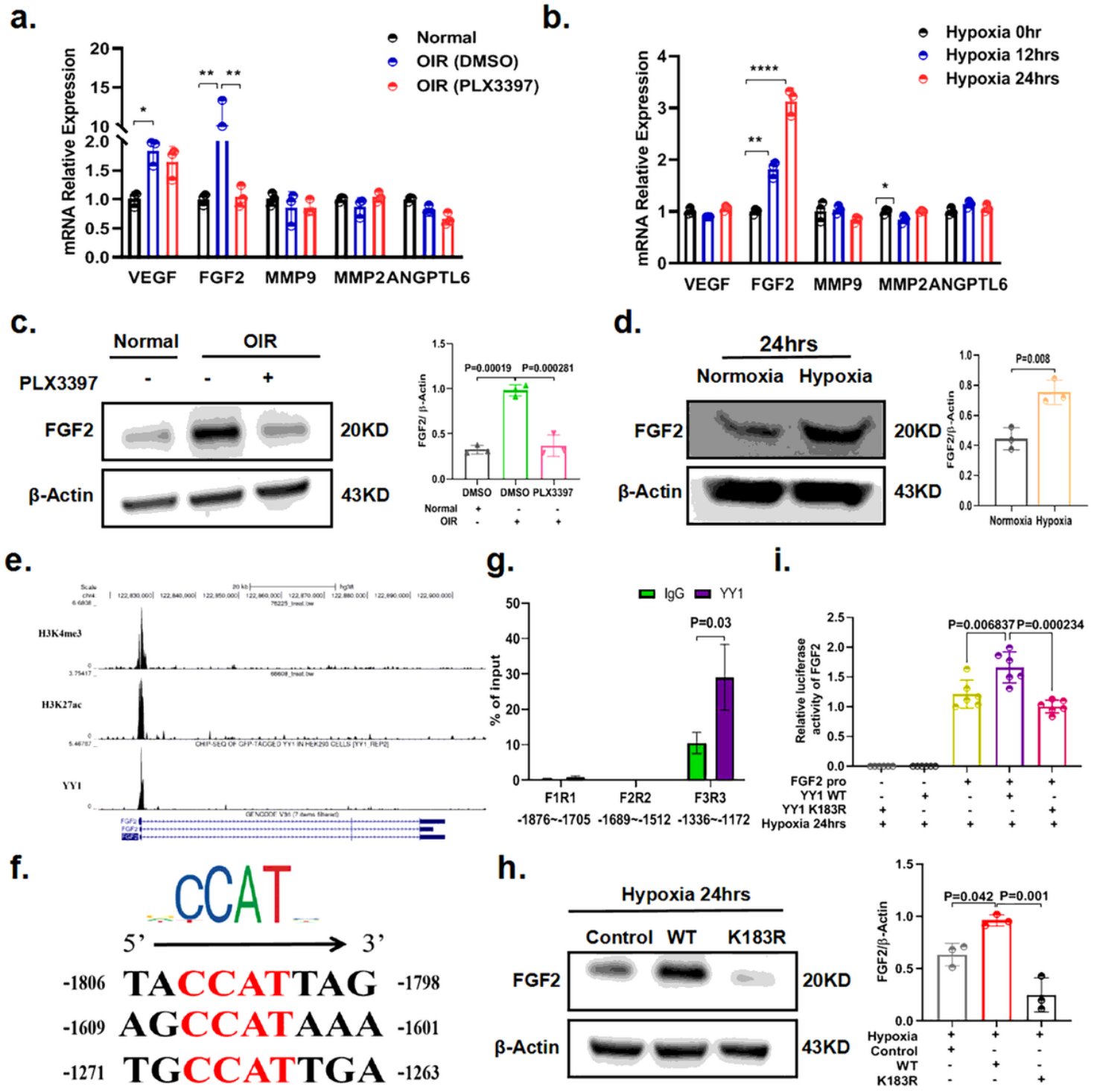

Figure 5

YY1 lactylation contributes to angiogenesis by regulating the expression of FGF2 (a) mRNA expression of VEGFA, FGF2, MMP2, MMP9 and ANGPTL6 in the retinal tissue of normal control (Normal P17) and OIR (OIR P17) mice by qRT-PCR. (b) mRNA expression of VEGFA, FGF2, MMP2, MMP9 and ANGPTL6 in HMC3 cells in the three groups subjected to hypoxia for 0 hr, 12 hrs and 24 hrs by qRT-PCR. (c) The expression of FGF2 in the retinas of normal control(normal), OIR (DMSO) and OIR (PLX3397) mice. (d) The expression of FGF2 in the HMC3 cells subjected to hypoxia for 0 hr and 24 hrs was analysed by Western blotting. (e) Genomic tracks for ChIP-seq around FGF2. (f) Potential YY1 binding sites of FGF2 promoter. (g) ChIP-qPCR analysis was performed with primers spanning predicted FGF2 promoter sequences. (h) The expression of FGF2 in HMC3 cells exposed to hypoxia 24 hrs (Hypoxia Control), hypoxia for 24 hrs+ YY1 WT transfection (Hypoxia+WT) and hypoxia for 24 hrs+YY1 K183R transfection (Hypoxia+K183R). (i) The luciferase activity of the FGF2 promoter (−1336 bp ~ − 1172 bp) driven reporter vector was measured in response to YY1 WT or K183R cotransfection under hypoxia. (n = 6; one-way ANOVA, Bonferroni test).

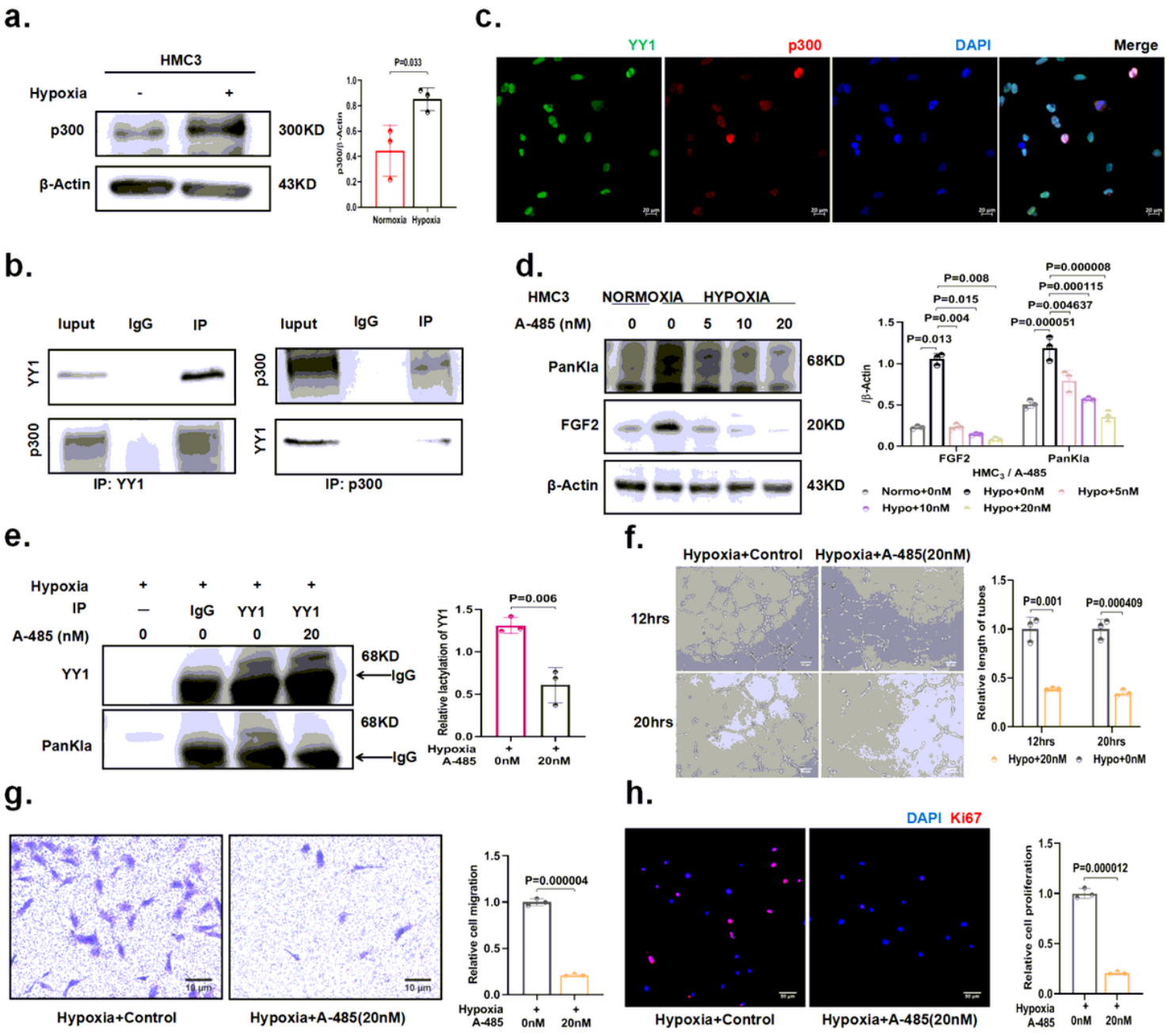

Figure 6

Inhibiting p300 reduces the lactylation of YY1 and suppresses angiogenesis (a) Quantification of p300 in the HMC3 cells under normoxia or hypoxia for 24 hrs. (b) Co-IP analysis of YY1 and p300. (c) Colocalization of YY1 and p300 by double-label immunofluorescence. (d)The expression of FGF2 and Pan-Kla in the HMC3 cells treated with 0 nM, 5 nM, 10 nM and 20 nM A-485 under hypoxia for 24hrs. (e)Applying A-485 decreased YY1 lactylation. Lactylation of YY1 with 0 nM A-485, or 20 nM A-485 was detected by Pan-Kla antibodies. (f-h) HMC3 cells were pretreated with DMSO or A485 for 24 hrs under hypoxia. Then HRMECs were cocultured with the pretreated HMC3 cells. The tube formation, migration and proliferation assays were performed as shown in the Methods.

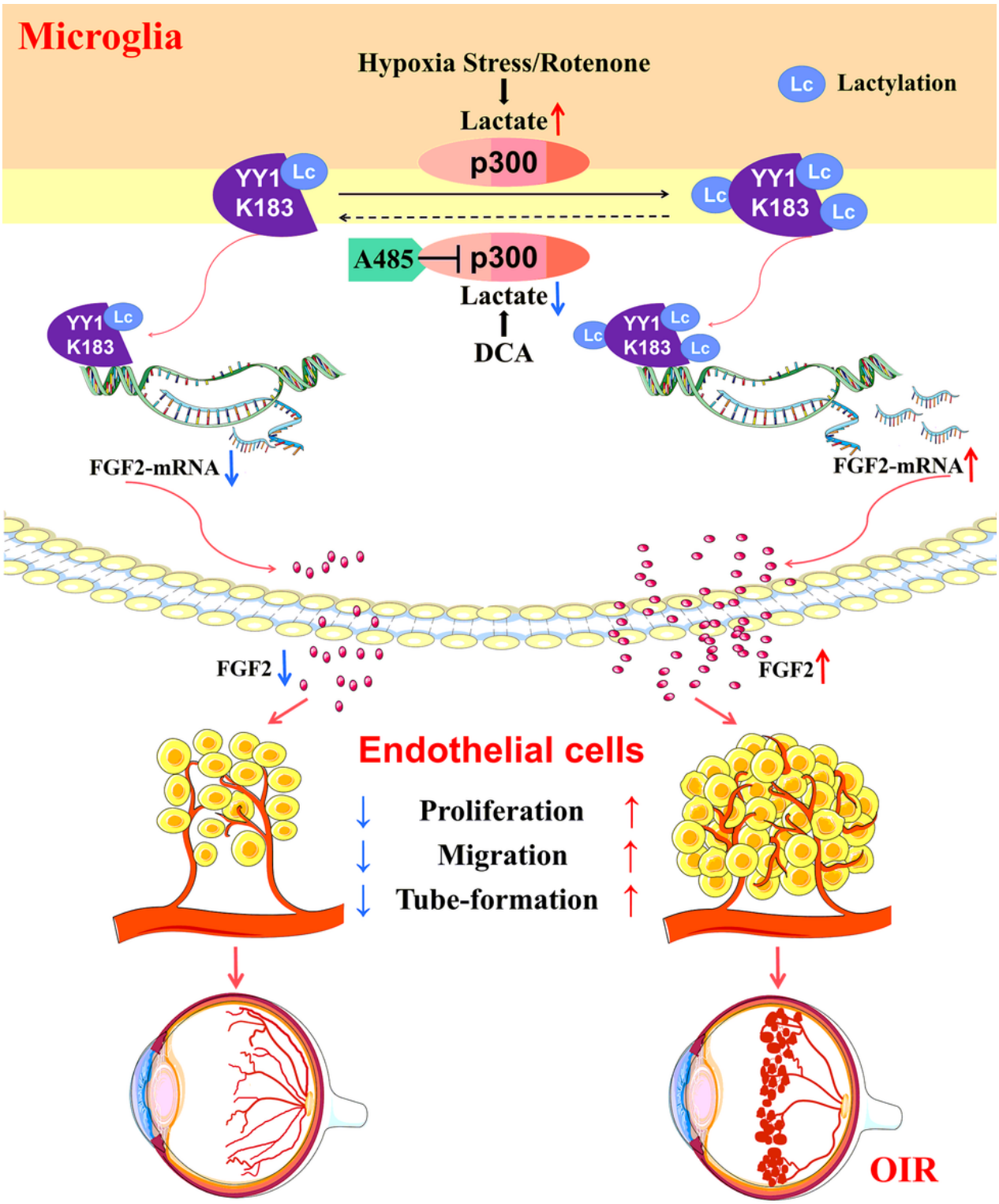

Figure 7

Figure legend not available with this version.

Supplementary Files

This is a list of supplementary files associated with this preprint. Click to download.

- nrreportingsummary1.pdf
- NCOMMS2136911DatasetAccessDetails.docx
- supplementaryfigures.docx
- supplementarytables.docx